

Joint theoretical and experimental study of the gas-phase elimination kinetics of *tert*-butyl ester of carbamic, *N,N*-dimethylcarbamic, *N*-hydroxycarbamic acids and 1-(*tert*-butoxycarbonyl)-imidazole

Jose R Mora,¹ María Tosta,¹ Rosa M. Domínguez,¹ Armando Herize,¹ Jenny Barroso,² Tania Córdova² and Gabriel Chuchani^{1*}

¹Centro de Química, Instituto Venezolano de Investigaciones Científicas (I.V.I.C.), Apartado 21827, Caracas, Venezuela

²Escuela de Química, Facultad de Ciencias, Universidad Central de Venezuela, Apartado 1020-A, Caracas, Venezuela

Received 8 February 2007; revised 4 June 2007; accepted 27 June 2007

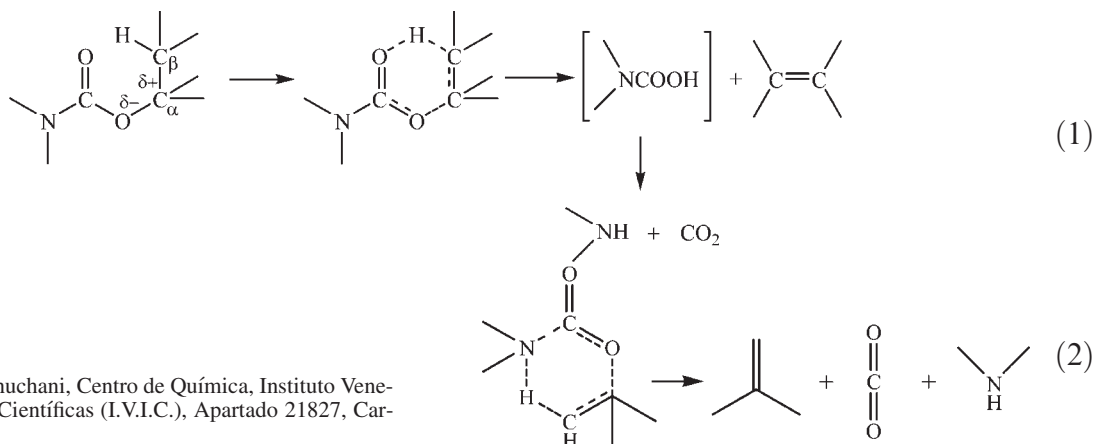
ABSTRACT: The gas-phase elimination kinetics of the title compounds were carried out in a static reaction system and seasoned with allyl bromide. The working temperature and pressure ranges were 200–280 °C and 22–201.5 Torr, respectively. The reactions are homogeneous, unimolecular, and follow a first-order rate law. These substrates produce isobutene and corresponding carbamic acid in the rate-determining step. The unstable carbamic acid intermediate rapidly decarboxylates through a four-membered cyclic transition state (TS) to give the corresponding organic nitrogen compound. The temperature dependence of the rate coefficients is expressed by the following Arrhenius equations: for *tert*-butyl carbamate $\log k_1$ (s^{-1}) = $(13.02 \pm 0.46) - (161.6 \pm 4.7) \text{ kJ/mol}(2.303 RT)^{-1}$, for *tert*-butyl *N*-hydroxycarbamate $\log k_1$ (s^{-1}) = $(12.52 \pm 0.11) - (147.8 \pm 1.1) \text{ kJ/mol}(2.303 RT)^{-1}$, and for 1-(*tert*-butoxycarbonyl)-imidazole $\log k_1$ (s^{-1}) = $(11.63 \pm 0.21) - (134.9 \pm 2.0) \text{ kJ/mol}(2.303 RT)^{-1}$. Theoretical studies of these elimination were performed at Møller–Plesset MP2/6-31G and DFT B3LYP/6-31G(d), B3LYP/6-31G(d,p) levels of theory. The calculated bond orders, NBO charges, and synchronicity (Sy) indicate that these reactions are concerted, slightly asynchronous, and proceed through a six-membered cyclic TS type. Results for estimated kinetic and thermodynamic parameters are discussed in terms of the proposed reaction mechanism and TS structure. Copyright © 2007 John Wiley & Sons, Ltd.

KEYWORDS: *tert*-butyl carbamates; kinetics; gas-phase elimination; MP2/6-31G; B3LYP/6-31G(d); B3LYP/6-31G(d,p) calculations; mechanism

INTRODUCTION

The gas-phase elimination of esters of *N,N*-dimethylcarbamic acids with a C_β–H bond at the alkyl side is generally considered to proceed through a six-membered cyclic transition state (TS) type of mechanism,

similar to those described for acetates, carbonates, and xanthates^{1–7} [reaction (1)]. A mechanism described in reaction (2) was thought to be possible.⁸ However, the same authors considered the TS for the β-H abstraction by nucleophilic nitrogen atom improbable.



*Correspondence to: G. Chuchani, Centro de Química, Instituto Venezolano de Investigaciones Científicas (I.V.I.C.), Apartado 21827, Caracas, Venezuela.

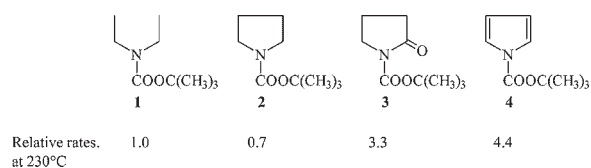
E-mail: chuchani@ivic.ve

The carbamate esters were also thought to decompose through an intermediate whose structure lies between a semi-concerted six-membered cyclic TS and an intimate ion-pair type of mechanism.^{7,9} Moreover, the elimination kinetics of 2-substituted alkyl ethyl *N,N*-diethyl carbamates¹⁰ showed a difference in the elimination rates of olefin formation in the order *tert*-butyl > isopropyl > ethyl. A similar sequence for the corresponding 2-substituted alkyl ethyl *N,N*-dimethyl carbamates¹¹ was obtained. The mechanism of these reactions was explained in terms of C α —O bond polarization, in the direction C $\alpha^{\delta+}$ —O δ^- , as a determining factor to proceed according to reaction (1).

Phenyl and bulky groups attached to the N atoms of ethyl carbamates were found to decrease the elimination rates due to steric factors.¹² The use of several correlation methods,¹³ such as the steric parameters of Hancock's E_s^c , Taft's E_s , Charton's ν , the inductive σ_I values, and the Taft–Topsom equation, for a large number of 2-substituted-ethyl *N,N*-dimethylcarbamates,¹⁴ (CH₃)₂NCOOCH₂CH₂Z, gave random points with no meaning for a reasonable mechanistic interpretation. However, the plot of the $\log k_Z/k_{CH_3}$ against the original Taft σ (values¹⁴ gave rise at the origin [$\sigma((CH_3)) = 0.00$] to three approximately straight lines. Such results suggested that small alterations in the polarity of the TS may be due to changes of electronic transmission at the reaction center. This means that a simultaneous effect may be operating during the process of elimination. A reasonable mechanism was proposed according to each slope of the straight lines. In the case of the point position of Z = phenyl (C₆H₅) and isopropenyl [CH₂=C(CH₃)], substituents falling far above the three lines were found to enhance the rate of elimination due to the acidity of the benzylic and allylic C β —H bond.¹⁵

A theoretical study using the Møller–Plesset MP2/6-31G method for the gas-phase elimination of 2-substituted alkyl ethyl *N,N*-dimethyl carbamate¹⁶ gave additional support for the concerted, non-synchronous six-membered cyclic TS mechanism. Correlation of the logarithm of the theoretical rate coefficients against Taft (ρ^* values gave an approximate straight line of $\rho^* = -1.39$, $r = 0.956$ at 360 °C¹⁶ in comparison of the experimental correlation of $\rho^* = -1.94$, $r = 0.976$ at 360 °C. It is interesting to note that the experimental $\log k_{rel}$ versus the theoretical $\log k_{rel}$ of these alkyl substituted carbamates gave a straight line ($r = 0.9919$ at 360 °C),¹⁶ implying similar mechanism.

Saturated heterocyclic carbamates¹⁷ showed a decrease in elimination rates due to electronic factors. The nitrogen atom of heterocyclic carbamates has its electrons delocalized through the pi bonds, causing a rate enhancement from the resonance interactions (Scheme 1). The elimination products of these carbamates are the corresponding carbamic acids and isobutylene. The intermediate acids are unstable and decarboxylate at the reaction temperature.



Scheme 1.

Recently, work related to the heterocyclic carbamates described above was examined theoretically at the MP2/6-31G level of theory.¹⁸ The theoretical thermodynamic and kinetic parameters were found to be in good agreement with the experimental values. TS structures are described as six-membered rings with some departure from planarity.

The previous investigations of comparable reactions have led to the examination of both experimental and theoretical elimination kinetics of *tert*-butyl carbamates with different substituents directly attached to the N atom, such as *tert*-butyl carbamate and *tert*-butyl *N,N*-dimethyl carbamate. These substrates may be useful to use for related or comparative study on the gas-phase decomposition of *tert*-butyl carbamates compounds. In the present paper, the kinetic work on the gas-phase elimination of *tert*-butyl *N*-hydroxycarbamate and 1-(*tert*-butoxycarbonyl)-imidazole is included.

COMPUTATIONAL METHODS AND MODELS

Electronic structure calculations were carried out using Møller–Plesset perturbation method MP2/6-31G and DFT B3LYP/6-31G(d), B3LYP/6-31G(d,p) as implemented in Gaussian 98W.¹⁹ The Berny analytical gradient optimization routines were used. The requested convergence on the density matrix was 10⁻⁹ atomic units, the threshold value for maximum displacement was 0.0018 Å, and that for the maximum force was 0.00045 Hartree/Bohr. The nature of stationary points was established by calculating and diagonalizing the Hessian matrix (force constant matrix). TS structures were characterized by means of normal-mode analysis. The transition vector (TV) associated with the unique imaginary frequency, that is, the eigenvector associated with the unique negative eigenvalue of the force constant matrix, has been characterized.

Frequency calculations were carried out to obtain thermodynamic quantities such as zero point vibrational energy (ZPVE), temperature corrections $E(T)$, and absolute entropies $S(T)$. Temperature corrections and absolute entropies were obtained assuming ideal gas behavior from the harmonic frequencies and moments of inertia by standard methods²⁰ at the average temperature and pressure values within the experimental range. Scaling factors for frequencies and zero point energies were taken from the literature.²¹

Method	f_{VIB}	f_{ZPE}
HF/6-31G(D)	0.8929	0.9135
B3LYP/6-31G(d)	0.9613	0.9804
B3LYP/6-311G(d,p)	0.97	0.99
MP2(Full)/6-31G(d)	0.9427	0.9676

The first-order rate coefficient $k(T)$ was calculated using the TST²² assuming that the transmission coefficient is equal to 1, as expressed in the following relation:

$$k(T) = (KT/h) \exp(-\Delta G^\ddagger/RT)$$

where ΔG^\ddagger is the Gibbs free energy change between the reactants and the TS and K and h are the Boltzmann and Planck constants, respectively. ΔG^\ddagger was calculated using the following relations:

$$\Delta G^\ddagger = \Delta H^\ddagger - T\Delta S^\ddagger$$

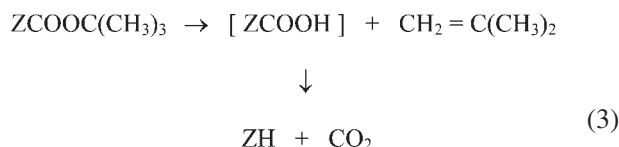
and

$$\Delta H^\ddagger = V^\ddagger + \Delta ZPVE + \Delta E(T)$$

where V^\ddagger is the potential energy barrier and $\Delta E(T)$ and $\Delta ZPVE$ are the differences of ZPVE and temperature corrections between the TS and the reactant, respectively.

RESULTS AND DISCUSSION

The molecular elimination of the carbamates described by reaction (3), in a static system,



with vessels seasoned with allyl bromide and in the presence of cyclohexene and/or toluene inhibitors,

demands that $P_f/P_0 = 3.0$, where the P_f and P_0 are the final and initial pressures, respectively. The average experimental results of P_f/P_0 values at four different temperatures and 10 half-lives were: 2.8 for *tert*-butyl carbamate, 2.9 for *tert*-butyl *N*-hydroxy carbamate, and 2.8 for 1-(*tert*-butoxycarbonyl)-imidazole (Table 1).

The small departure from $P_f = 3P_0$ may be due to slight polymerization of the product isobutene. Additional examination of the stoichiometry of reaction (3), up to 65–80% decomposition, was possible by comparing the percentage decomposition of the substrate calculated from pressure measurements with that obtained from the chromatographic analyses of the olefin product isobutene (Table 2).

To examine the influence of the surface area on the rate of elimination, several runs were carried out in a vessel with a surface-to-volume ratio 6.0 times greater than that normal which is equal to 1.0. The packed and unpacked clean Pyrex vessels, except 1-(*tert*-butoxycarbonyl)-imidazole had a significant effect on the rates. However, the packed and unpacked vessels seasoned with allyl bromide showed no marked effect on the rate coefficients of these carbamates (Table 3). The pyrolysis of these carbamates, in seasoned vessels, had to be carried out in the presence of at least twice the amount of the inhibitor cyclohexene and/or toluene (Table 4). No induction period was obtained. The rate coefficients are reproducible with a relative standard deviation not greater than 5% at a given temperature.

The rate coefficient of these eliminations has been found to be independent of initial pressures (Table 5), and the first-order rate coefficient was calculated from $\ln(3P_0 - P_t)$. A plot of $\log(3P_0 - P_t)$ against time (t) gave a good straight line up to 65–80% decomposition (Fig. 1). The variation of the rate coefficient with temperature and the corresponding Arrhenius equations are given in Table 6 (90% confidence coefficient from least-squares procedure).

To provide a reasonable mechanism from the calculated results of Table 7 describing the elimination kinetics *tert*-butyl carbamates, a theoretical examination was carried out.

Table 1. Ratio of final (P_f) to initial pressure (P_0) of the substrate

Substrate	Temperature (°C)	P_0 (Torr)	P_f (Torr)	P_f/P_0	Aver.
<i>tert</i> -Butyl carbamate	249.0	35	96.5	2.8	2.8
	261.5	33	90.5	2.7	
	270.8	26	72	2.8	
	280.9	39	107.5	2.8	
<i>tert</i> -Butyl <i>N</i> -hydroxy carbamate	219.0	76	222.5	2.9	2.9
	230.4	49	144	3.0	
	240.3	67.5	199.5	2.9	
	250.3	68	200	2.9	
	250.3	68	200	2.9	
1-(<i>tert</i> -Butoxycarbonyl)-imidazole	198.3	20.3	53.6	2.6	2.8
	216.7	16.8	46.8	2.8	
	226.6	26.2	74.2	2.8	
	238.1	27.9	76.7	2.8	

Table 2. Stoichiometry of the reaction

Substrate	Temperature (°C)	Parameters	Value				
<i>tert</i> -Butyl carbamate	261.5	Time (min)	3	4	8	12	
		Reaction (%) (pressure)	26.8	34.2	56.6	71.1	
		Isobutene (%) (GLC)	27.6	33.2	53.5	75.0	
<i>tert</i> -Butyl <i>N</i> -hydroxy carbamate	229.3	Time (min)	1	3	7	10	14
		Reaction (%) (pressure)	7.9	19.1	42.7	56.2	67.4
		Isobutene (%) (GLC)	7.1	18.8	41.9	56.8	69.9
1-(<i>tert</i> -Butoxycarbonyl)-imidazole	216.7	Time (min)	3.6	7	8.5	12	18.5
		Reaction (%) (pressure)	27.6	45.7	58.7	78.4	86.7
		Isobutene (%) (GLC)	24.8	42.5	55.2	75.7	83.0

Table 3. Homogeneity of the reactions

Compound	S/V (cm ⁻¹)	$10^4 k_1$ (s ⁻¹) ^a	$10^4 k_1$ (s ⁻¹) ^b
<i>tert</i> -Butyl carbamate at 249.0 °C	1	14.15	7.93
	6	13.79	7.42
<i>tert</i> -Butyl <i>N</i> -hydroxy carbamate at 219.4 °C	1	11.43	7.03
	6	13.39	7.15
1-(<i>tert</i> -Butoxycarbonyl)-imidazole at 216.4 °C	1	18.00	17.74
	6	16.77	17.23

S = surface area; V = Volume.

^aClean Pyrex vessel.

^bVessel seasoned with allyl bromide.

Table 4. Effect of the free radical inhibitor on rates

Substrate	Temperature (°C)	P_s (Torr)	P_i (Torr)	P_i/P_s	$10^4 k_1$ (s ⁻¹)
<i>tert</i> -Butyl carbamate ^c	249.0	34.5	—	—	7.97
		51.5	51	1.0	7.65
		35	61.5	1.8	8.08
		23	100.5	4.4	7.96
		19	101	5.2	8.00
<i>tert</i> -Butyl <i>N</i> -hydroxy carbamate ^a	219.3	55	—	—	10.93
		58.3	44	0.8	7.68
		80.3	115	1.4	7.77
		53	106.5	2.0	7.87
1-(<i>tert</i> -Butoxycarbonyl)-imidazole ^b	216.6	74	—	—	15.21
		41.5	59	1.4	19.21
		42	86	2.1	18.00
		42	126	3.0	19.16

P_s = pressure of the substrate.

P_i = Pressure of the inhibitor.

^aToluene inhibitor.

^bCyclohexene inhibitor.

Table 5. Invariability of the rate coefficients with initial pressure

Substrate	Temperature (°C)	Parameters	Value				
<i>tert</i> -Butyl carbamate	249.0	P_0 (Torr)	19	24	34.5	51.5	
		$10^4 k_1$ (s ⁻¹)	8.00	7.86	7.97	7.60	
<i>tert</i> -Butyl <i>N</i> -hydroxy carbamate	219.3	P_0 (Torr)	53	80.3	94	127	
		$10^4 k_1$ (s ⁻¹)	7.87	7.77	7.67	7.45	
1-(<i>tert</i> -Butoxycarbonyl)-imidazole	226.6	P_0 (Torr)	22.9	36.2	46	56	64
		$10^4 k_1$ (s ⁻¹)	34.29	33.12	33.42	33.71	34.04

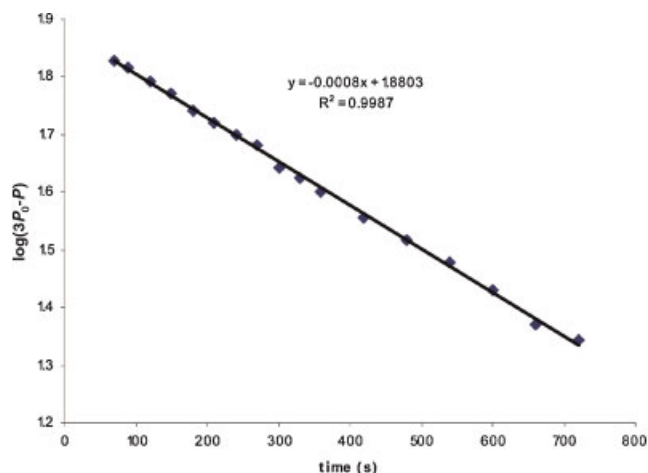


Figure 1. A representative plot of $\log(3P_0 - P_t)$ versus time for carbamates (*tert*-butyl carbamate at 261.5 °C). This figure is available in colour online at www.interscience.wiley.com/journal/poc

Calculated kinetic and thermodynamic parameters

The gas-phase thermal decomposition of *N*-substituted *t*-butyl carbamates yields isobutylene and the corresponding carbamic acid in a slow step according to Scheme 2. The carbamic acids are unstable under the reaction conditions and decarboxylate rapidly to give carbon dioxide and the corresponding amine. The kinetics of the rate-determining step in the decomposition of *N*-substituted *t*-butyl carbamates as well as the decarboxylation of the corresponding carbamic acids were examined using electronic structure calculations.

Geometries for reactants, TS, and products for the reactions under study were optimized using Møller–Plesset perturbation MP2/6-31G and DFT B3LYP/6-31G(d), B3LYP/6-31G(d,p). Frequency calculations were carried out at the average experimental conditions for this series of *N*-substituted carbamates ($T = 230$ °C). Thermodynamic quantities such as ZPVE, temperature corrections ($H(T)$), energy, enthalpy, and free energies were obtained from vibrational analysis. Entropy values were calculated from vibrational analysis and using the empirical parameter C^{exp} suggested by Chuchani–Cordova.²³ This parameter is obtained from the experimental free energy of activation for each reaction and serves as scaling factor. The calculation results for the rate controlling step are shown in Table 8.

Analysis of calculated parameters at MP2/6-31G, B3LYP/6-31G(d), and B3LYP/6-31G(d,p) levels of theory shows that calculated activation energies are in reasonable agreement to the experimental counterparts for the two step mechanism at B3LYP/6-31G(d,p) level of theory [reaction (1)]. In all cases, MP2/6-31G overestimates the activation parameters, while DFT B3LYP/6-31G underestimates; however, the inclusion of polarization functions significantly improves the results as expected. Rate coefficients are within the same order of magnitude compared to experimental values. Experimentally, it is observed that the reaction is faster for the imidazole substituent followed by that of —NHOH, dimethylamine, and amine, that is: $\text{N}_2\text{C}_3\text{H}_3 > \text{NHOH} > \text{N}(\text{CH}_3)_2 > \text{NH}_2$. Calculated energies of activation follow the same trend.

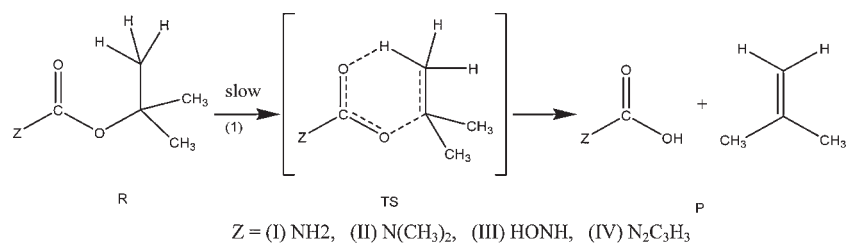
Calculated values of entropies of activation for the rate-determining step vary from -35 to -9 J/mol K. It

Table 6. Variation of rate coefficients with temperature

Substrate	Parameters	Value					
<i>tert</i> -Butyl carbamate	Temp. (°C)	235.6	240.1	249.0	261.5	270.8	280.8
	$10^4 k_1$ (s ⁻¹)	2.41	3.71	7.93	17.31	29.55	59.55
	Rate equation $\log k_1$ (s ⁻¹) =	$(13.02 \pm 0.46) - (161.6 \pm 4.7) \text{ kJ/mol} (2.303 RT)^{-1} r = 0.9983$					
<i>tert</i> -Butyl <i>N</i> -hydroxy carbamate	Temp. (°C)	220.3	210.3	219.4	230.4	239.8	250.3
	$10^4 k_1$ (s ⁻¹)	1.67	3.52	7.03	16.03	30.36	58.38
	Rate equation $\log k_1$ (s ⁻¹) =	$(12.52 \pm 0.11) - (147.8 \pm 1.1) \text{ kJ/mol} (2.303 RT)^{-1} r = 0.9999$					
1-(<i>tert</i> -Butoxycarbonyl)-imidazole	Temp. (°C)	198.3	207.5	216.7	226.6	238.1	
	$10^4 k_1$ (s ⁻¹)	4.84	9.26	18.00	34.12	64.10	
	Rate equation $\log k_1$ (s ⁻¹) =	$(11.63 \pm 0.21) - (134.9 \pm 2.0) \text{ kJ/mol} (2.303 RT)^{-1} r = 0.9998$					

Table 7. Kinetic and thermodynamics parameters for pyrolysis of ZCOOC(CH₃)₃ at 230.0 °C

Z	$k_1 \times 10^{-4}$ (s ⁻¹)	Ea (kJ/mol)	logA (s ⁻¹)	ΔS^\ddagger (J/mol K)	ΔH^\ddagger (kJ/mol)	ΔG^\ddagger (kJ/mol)	Ref.
NH ₂	1.74	161.6 ± 4.7	13.02 ± 0.46	-8.28	157.4	161.6	This work
(CH ₃) ₂ N	2.95	157.9	12.87	-11.15	153.7	159.3	11
HONH	14.79	147.8 ± 1.1	12.52 ± 0.11	-17.85	143.6	152.6	This work
C ₃ H ₃ N ₂	41.89	134.9 ± 2.0	11.63 ± 0.21	-34.89	130.7	148.3	This work



Scheme 2.

Table 8. Kinetic and thermodynamic parameters for the gas-phase elimination of *tert*-butyl carbamates Z-COO-C(CH₃)₃

Z	ΔH^\ddagger (kJ/mol)	E _a (kJ/mol)	ΔG^\ddagger (kJ/mol)	ΔS^\ddagger (J/mol K)	logA (s ⁻¹)	$k \times 10^4$ (s ⁻¹)
-NH ₂	157.4 ^a	161.6 ^a	161.6 ^a	-8.28 ^a	13.02 ^a	1.74 ^a
	175.3 ^b	179.5 ^b	174.7 ^b	1.19 ^b	13.51 ^b	0.07 ^b
	134.3 ^c	138.5 ^c	138.5 ^c	-8.35 ^c	13.02 ^c	439 ^c
	151.5 ^d	155.6 ^d	155.6 ^d	-8.15 ^d	13.03 ^d	7.41 ^d
-N(CH ₃) ₂	153.7 ^a	157.9 ^a	159.3 ^a	-11.15 ^a	12.87 ^a	2.95 ^a
	162.3 ^b	166.6 ^b	167.6 ^b	-10.40 ^b	12.91 ^b	0.42 ^b
	130.6 ^c	134.8 ^c	136.2 ^c	-11.09 ^c	12.88 ^c	759 ^c
	148.7 ^d	152.9 ^d	154.3 ^d	-11.11 ^d	12.87 ^d	10.0 ^d
-NHOH	143.6 ^a	147.8 ^a	152.6 ^a	-17.85 ^a	12.52 ^a	14.8 ^a
	156.4 ^b	160.5 ^b	165.2 ^b	-17.70 ^b	12.53 ^b	0.74 ^b
	126.2 ^c	130.4 ^c	135.2 ^c	-17.95 ^c	12.52 ^c	964 ^c
	141.0 ^d	145.2 ^d	150.0 ^d	-17.83 ^d	12.52 ^d	28.0 ^d
-N ₂ C ₃ H ₃	130.7 ^a	134.9 ^a	148.3 ^a	-34.89 ^a	11.63 ^a	41.89 ^a
	147.0 ^b	151.1 ^b	164.1 ^b	-34.80 ^b	11.63 ^b	0.96 ^b
	120.7 ^c	124.9 ^c	138.3 ^c	-34.98 ^c	11.63 ^c	460 ^c
	134.9 ^d	139.1 ^d	152.5 ^d	-35.02 ^d	11.63 ^d	15.4 ^d

Z = NH₂, N(CH₃)₂, NHOH, and N₂C₃H₃ calculated at 230 °C

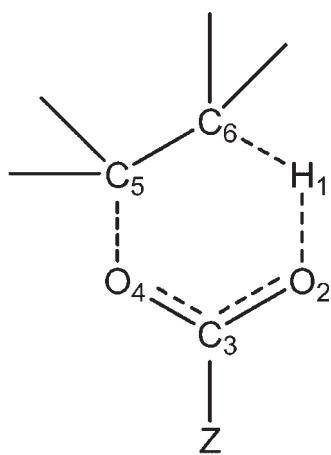
^a Experimental.

^b MP2/6-31G.

^c B3LYP/6-31G.

^d B3LYP/6-31G(d,p).

is interesting that the more constrained TS corresponds to the fastest reaction: N₂C₃H₃ > NHOH > N(CH₃)₂ > NH₂; that is, the loss of degrees of freedom in the TS is compensated by activation energies which vary in the sense N₂C₃H₃ < NHOH < N(CH₃)₂ < NH₂. The negative activation entropies are indicative of a concerted process and a cyclic TS geometry (Scheme 3, Fig. 2). The TS for the gas-phase thermal decomposition of *N*-substituted *t*-butyl carbamates is a cyclic six-membered structure, in accord to logA values between 11.63 and 13.02.²⁴



Scheme 3.

Parameters for decarboxylation of the intermediate *N*-substituted carbamic acids were also calculated at the B3LYP/6-31G level of theory. Experimentally, this was not possible due to instability of the acids under the reaction conditions. Calculated energies of activation and rate coefficients for this step are shown in Table 9. The TS for this step is shown in Fig. 3. Calculated energies of activation and rate coefficients demonstrate that decarboxylation of the carbamic acids is significantly faster than the previous step for all substrates.

An alternate pathway [reaction (2)] was also investigated. This mechanism is unlikely because the lone electron pair on the nitrogen is involved in a partial double bond with the carbonyl oxygen in the carbamates, as seen on optimized carbamate structures. Even though the electron density on the nitrogen is significant, proton affinity on amides shows that the carbonyl oxygen is more likely to be protonated than the nitrogen, thereby suggesting that the abstraction is carried out by the carbonyl oxygen. Previous theoretical studies on similar substrates support the mechanism shown in reaction (1), Scheme 2.^{16,18} Calculated activation parameters for the mechanism in reaction (2) for *t*-butyl carbamate (Z = NH₂) calculated at B3LYP/6-31G(d) are: $\Delta H^\ddagger = 207.67$ kJ/mol, E_a = 211.85 kJ/mol, $\Delta G^\ddagger = 203.84$ kJ/mol, $\Delta S^\ddagger = 7.61$ J/K mol. Activation parameters for the

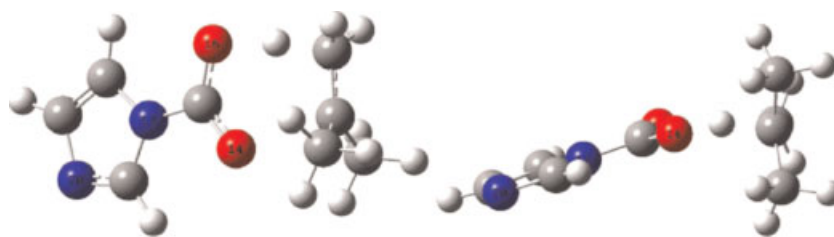


Figure 2. Two views of the optimized structures for the TS in the rate-determining step are shown for Z = imidazole. TS geometries are a six-membered ring for all carbamates in this series. The six atoms involved in are almost in the same plane (O–C–O–C–C–H). The imaginary frequency is associated with the transfer of the hydrogen from C β at the ester side of the carbamate to the carbonyl oxygen. This figure is available in colour online at www.interscience.wiley.com/journal/poc

Table 9. Energies of activation and rate coefficients for N-substituted carbamic acids decarboxylation step from B3LYP/6-31G(d) calculations

Z	k_2 (10^{-4} s^{-1})	Ea (kJ/mol)
N(CH ₃) ₂	1995931.7	98.3
NH ₂	481115.4	102.6
HONH	54795.0	116.0
N ₂ C ₃ H ₃	16582.3	121.2

N-substituted carbamic acids are intermediates in the thermal decomposition of *tert*-butyl carbamates Z-COO-C(CH₃)₃ at 230 °C.

mechanism in reaction (2) deviate significantly from experimental values; the energy of activation is about 50 kJ/mol higher than experimental. These findings suggest that the thermal decomposition of *t*-butyl carbamates proceeds through the mechanism in reaction (1) as proposed in previous investigations.^{16,18}

TS structure and mechanism

Geometrical parameters for reactants and TSs of the rate-determining step for mechanism in reaction (1) are shown in Table 10. Distances and angles between the atoms involved in the reaction (H1, O2, C3, O4, C5, and C6) show that the TS geometry is a six-membered ring with the hydrogen being transferred (H1) midway between the carbon (C6) and the oxygen (O2) (Scheme 3, Fig. 2). The TS structure is almost planar for all carbamates, except when Z = —NHOH, for which

some departure from planarity was observed in the dihedral angles.

Comparison of TS structure for the carbamates of this series showed similarity in bond distances. However, some differences were observed; for example, the progress in H1—O2 bond forming is more advanced for carbamate Z = NH₂. The O4—C5 bond is more elongated for the TS of carbamate Z = N₂C₂H₃ in the TS. Some changes are observed also in C6—H1 bond breaking, indicating differences in the electronic density distribution in the TS for this series of carbamates. The TS C6—H1 bond breaking distance is longer (1.270 Å) for carbamates Z = NH₂ and Z = N(CH₃)₂ compared to 1.230 Å for carbamates Z = NHOH and Z = N₂C₂H₃. Conversely, the breaking of O4—C5 bond is more advanced for carbamate Z = N₂C₂H₃. The progress of the reaction in the TS shows that O4—C5 and C6—H1 bond distances increase implying breaking of these bonds (1.47–1.48 to 2.15–2.90 Å in TS and 1.08–1.09 to 1.23–1.27 Å in TS, respectively). The C5—C6 and C3—O4 bond distances reveal changes from single to double bond character (1.53 to 1.41 Å in TS and 1.33–1.35 to 1.25–1.27 Å in TS, respectively) as hybridization changes from sp³ to sp². The transition vector TV shows that the process is dominated by the elongation of O4—C5 bond.

TSs for the rate-determining step were characterized by unique imaginary frequencies: –1061.1, –1047.5, –748.6, and –705.4 cm⁻¹ for Z = NH₂, N(CH₃)₂, NHOH, and N₂C₃H₃ respectively, and it is associated with the displacement of hydrogen H1 from C6 to the carbonyl oxygen O2. It is interesting that the imaginary frequency is much lower for carbamates Z = NHOH and N₂C₃H₃.

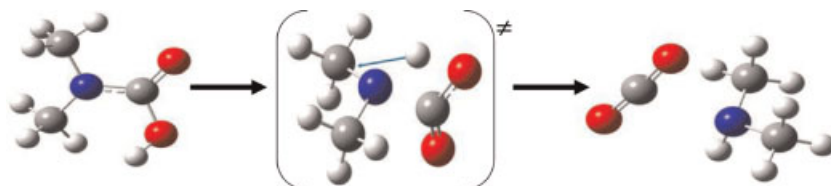


Figure 3. Decarboxylation reaction of the unstable N-substituted carbamic acids. The TS structure is a four-membered ring (N–C–O–H) and the imaginary frequency is associated with the hydrogen transfer. This figure is available in colour online at www.interscience.wiley.com/journal/poc

Table 10. Structural parameters reactants (R), TS, and products (P) for *tert*-butyl carbamates Z-COO-C(CH₃)₃;

	Atom distances (Å)						
	H ₁ -O ₂	O ₂ -C ₃	C ₃ -O ₄	O ₄ -C ₅	C ₅ -C ₆	C ₆ -H ₁	C ₃ -N ₇
				Z = -NH ₂			
R	2.414	1.210	1.350	1.470	1.530	1.090	1.365
TS	1.278	1.280	1.270	2.150	1.410	1.270	1.377
P	0.979	1.350	1.220	3.400	1.340	2.310	1.360
				Z = -N(CH ₃) ₂			
R	2.397	1.220	1.350	1.470	1.530	1.080	1.372
TS	1.351	1.280	1.270	2.140	1.410	1.270	1.377
P	0.979	1.350	1.220	3.390	1.340	2.310	1.365
				Z = -NHOH			
R	3.503	1.210	1.330	1.470	1.530	1.090	1.396
TS	1.419	1.270	1.270	2.230	1.410	1.230	1.393
P	0.983	1.330	1.220	3.410	1.340	2.220	1.373
				Z = -N ₂ C ₃ H ₃			
R	2.445	1.210	1.330	1.480	1.530	1.090	1.410
TS	1.434	1.260	1.250	2.290	1.410	1.230	1.426
P	0.986	1.330	1.210	3.410	1.340	2.180	1.403
				Dihedral angles (degrees)			
	H ₁ -O ₂ -C ₃ -O ₄	O ₂ -C ₃ -O ₄ -C ₅	C ₃ -O ₄ -C ₅ -C ₆	O ₄ -C ₅ -C ₆ -H ₁			
				Z = -NH ₂			
TS	-5.699	7.210		-3.820			-0.050
				Z = -N(CH ₃) ₂			
TS	1.300	-1.530		0.680			0.130
				Z = -NHOH			
TS	-14.480	16.390		-6.590			-1.540
				Z = -N ₂ C ₃ H ₃			
TS	-0.260	0.300		-0.060			-0.120
				Imaginary frequency (cm ⁻¹)			
	NH ₂	N(CH ₃) ₂	NHOH	N ₂ C ₃ H ₃			
TS	-1061.1	-1047.5	-748.6	-705.4			

Z = NH₂, N(CH₃)₂, NHOH, and N₂C₃H₃.

Atom distances are in Å and dihedral angles are in degrees from B3LYP/6-31G(d,p) calculations.

NBO charges in Table 11 show the changes in electron density for each substrate, from the reactant structure (R) to the TS of the rate-determining step (TS) to products (P). In all substrates there is an important charge separation in atoms C₃-O₂ (carbonyl moiety), C₃-O₄, and O₄-C₅.

The analysis illustrates that O₄-C₅ bond is highly polarized in the reactants and the charge separation increases in the TS structures, in the sense O₄^{δ-}-C₅^{δ+}. Following the reaction coordinate from reactant to TS, the following changes in partial charges occur: an increase in positive charge δ+ in hydrogen H₁ (from 0.11-1.45 to 0.331, 0.344 in TS), a small increase in negative charge in carbonyl oxygen O₂ (-0.488, -0.539 to -0.563, -0.594 in TS), and an increase in negative charge in O₄ (-0.495, -0.535 to -0.561, -0.597 in TS). There is also an increase in the polarization at the O₄-C₅ bond, with charge separation increasing from 0.77, 0.76 in the reactants to 0.82, 0.85 in the TS. The more polarized TS is

that of carbamates Z = NHOH and N₂C₃H₃. The observation on NBO charges together with rate coefficients implies that the alkyl oxygen-carbon bond polarization in the sense O^{δ-}-C^{δ+}, dominates the decomposition process. Charge density plots of the TS (Fig. 4) show the polarization towards the substituents -NHOH and N₂C₃H₃.

Bond order analysis

Bond order calculations NBO were performed.²⁵⁻²⁷ Wiberg²⁸ bond indexes were computed using the natural bond orbital NBO program²⁹ as implemented in Gaussian 98W, to further investigate the nature of the TS along the reaction pathway. Bond breaking and making processes involved in the reaction mechanism can be monitored by means of the Synchronicity (Sy) concept proposed by

Table 11. NBO charges for reactants (R), TS, and products (P) for *tert*-butyl carbamates Z-COO-C(CH₃)₃

	NBO charges					
	R	TS	P	R	TS	P
	Z = -NH ₂			Z = -N(CH ₃) ₂		
H ₁	0.145	0.342	0.330	0.145	0.344	0.329
O ₂	-0.520	-0.572	-0.519	-0.539	-0.594	-0.534
C ₃	0.776	0.731	0.710	0.814	0.784	0.745
O ₄	-0.521	-0.566	-0.513	-0.535	-0.586	-0.533
C ₅	0.272	0.254	0.159	0.275	0.255	0.160
C ₆	-0.321	-0.463	-0.319	-0.321	-0.463	-0.319
N ₇	-0.620	-0.479	-0.483	-0.467	-0.448	-0.440
	Z = -NHOH			Z = -N ₂ C ₃ H ₃		
H ₁	0.110	0.331	0.334	0.146	0.331	0.336
O ₂	-0.510	-0.571	-0.514	-0.488	-0.563	-0.506
C ₃	0.788	0.744	0.728	0.823	0.773	0.756
O ₄	-0.495	-0.597	-0.529	-0.511	-0.561	-0.479
C ₅	0.263	0.257	0.157	0.258	0.258	0.156
C ₆	-0.323	-0.454	-0.328	-0.324	-0.455	-0.332
N ₇	-0.334	-0.278	-0.256	-0.505	-0.473	-0.463

Z = NH₂, N(CH₃)₂, NH₂OH, and N₂C₃H₃ from B3LYP/6-31G(d,p) calculations.

Moyano *et al.*³⁰ defined by the expression:

$$S_y = 1 - \frac{\sum_{i=1}^n |\delta B_i - \delta B_{av}| / \delta B_{av}}{2n - 2}$$

n is the number of bonds directly involved in the reaction and the relative variation of the bond index is obtained

from:

$$\delta B_i = \frac{[B_i^{TS} - B_i^R]}{[B_i^P - B_i^R]}$$

where the superscripts R, TS, P, represent reactant, TS, and product, respectively.

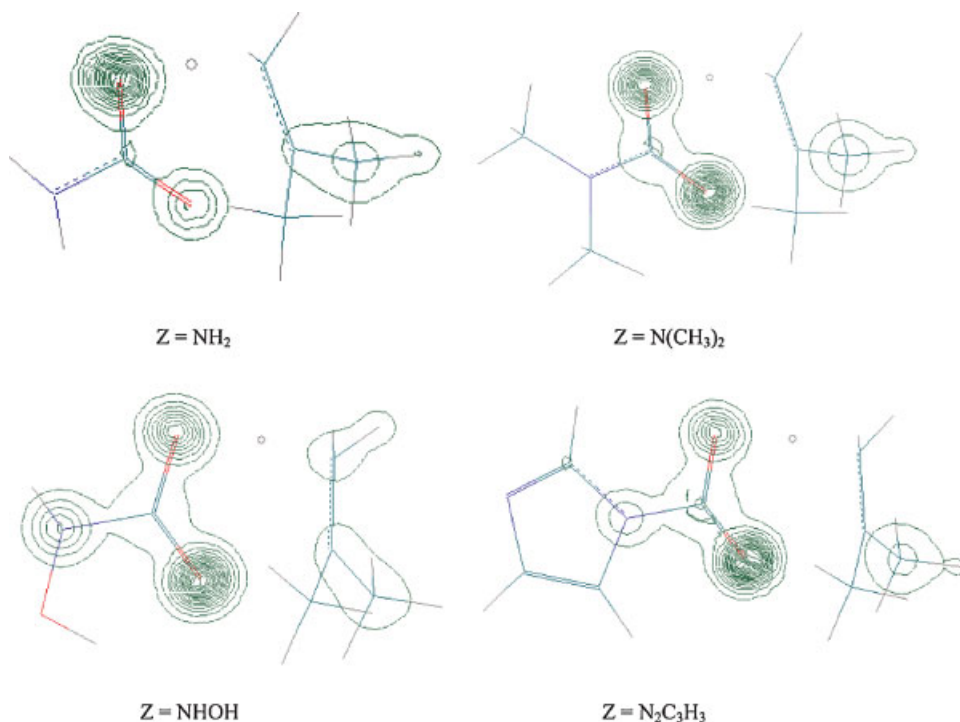


Figure 4. Charge density plots the TS in carbamate Z-COO-C(CH₃)₃; Z = NH₂, N(CH₃)₂, NHOH, and N₂C₃H₃. Polarization of the electron density toward the substituents NHOH and N₂C₃H₃ is observed. This figure is available in colour online at www.interscience.wiley.com/journal/poc

The evolution in bond change is calculated as:

$$\%E_v = \delta B_i \times 100$$

The average value is calculated from:

$$\delta B_{\text{ave}} = \frac{1}{n} \sum_{i=1}^n \delta B_i$$

Bonds indexes were calculated for those bonds that change as the reaction proceeds, that is: H1—O2, O2—C3, C3—O4, O4—C5, C5—C6, C6—H1 (Scheme 3, Fig. 2); all other bonds remain practically unaffected. C3—N7 bond order was also included to investigate the possible participation in the reaction coordinate.

Calculated Wiberg indexes B_i for reactant, TS, and products for N-substituted *t*-butyl carbamates ($Z = -\text{NH}_2, -\text{N}(\text{CH}_3)_2, -\text{NHOH}, -\text{N}_2\text{C}_3\text{H}_3$) allow inspection of the progress of the reaction and the position of the TS between reactant and product (Table 12). Wiberg indexes show that for all carbamates in this series the most advanced reaction coordinate is O4—C5 bond breaking (68–76%), followed by C3—O4 bond change from single to double (55–61%). The O2—C3 change from double to single bond is intermediate (50–53%) indicating that hydrogen being transferred is halfway between O2 and C6. The advancement in other reaction coordinates is less important C6—H1 (43–48%), C5—C6 bond changes from single to double (35–37%) and H1—O2 (35–40%). The C3—N7 bond order shows very small changes. These results show that the most important event in the decomposition reaction is the polarization of alkyl

oxygen—carbon (O4—C5) bond leading to its breaking as the reaction proceeds, for all carbamates in the series. Sy parameters tell a concerted asynchronous, semipolar process, with Sy values ranging from 0.85 (most asynchronous, imidazole substituent) to 0.89 (less asynchronous, $Z = -\text{NH}_2, \text{N}(\text{CH}_3)_2$). The bond order analysis is in accord with the TS structure, both in distances, angles, and NBO charges as analyzed above. The TS structure shows more progress in O3—C4 bond breaking compared to other reaction changes. This finding suggests that the polarization of this bond in the sense $\text{O}3^{\delta-} - \text{C}4^{\delta+}$ is a determining factor in the gas-phase elimination of N-substituted *t*-butyl carbamates.

EXPERIMENTAL

Tert-butyl carbamate, *tert*-butyl *N*-hydroxycarbamate, and 1-(*tert*-butoxycarbonyl)-imidazole were bought from Aldrich. The purity and identity of the substrates and products were determined by GLC/MS (Saturn 2000, Varian). Capillary column DB-5MS, 30 mm × 0.250 mm., i.d. 0.25 μm. The olefin product isobutylene was analyzed using a chromatograph Varian 3700 with a flame ionization detector and a two meter packed column Porapak Q column (80–100 meshes).

Kinetics

The kinetics determinations were carried out in a static reaction system as described before.^{31–33} The reaction

Table 12. Wiberg bond index from NBO B3LYP/6-31G(d,p) calculations for reactant (R), TS, and products (P) for the thermal decomposition of *tert*-butyl carbamates $Z\text{-COO-C}(\text{CH}_3)_3$

	H1—O2	O2—C3	C3—O4	O4—C5	C5—C6	C6—H1	C3—N7	δB_{av}	S_y
					$Z = -\text{NH}_2$				
B_i^{R}	0.0056	1.647	0.9947	0.8215	1.0049	0.9096	1.1643	0.5071	0.8935
B_i^{ET}	0.2762	1.3182	1.3659	0.2649	1.3294	0.4854	1.1342		
B_i^{P}	0.6725	1.0274	1.6327	0.0014	1.8882	0.0226	1.1679		
$\%E_v$	40.58	53.07	58.18	67.87	36.74	47.82			
					$Z = -\text{N}(\text{CH}_3)_2$				
B_i^{R}	0.0057	1.6165	0.9905	0.8196	1.0046	0.909	1.1408	0.5047	0.8937
B_i^{ET}	0.274	1.2985	1.3405	0.2676	1.3272	0.4863	1.1220		
B_i^{P}	0.6692	1.0218	1.6012	0.0014	1.8888	0.0221	1.1465		
$\%E_v$	40.44	53.47	57.31	67.47	36.48	47.66			
					$Z = -\text{NHOH}$				
B_i^{R}	0.0001	1.6547	1.0365	0.8113	1.0062	0.9255	1.0878	0.4922	0.8718
B_i^{ET}	0.2383	1.3522	1.3422	0.2156	1.3165	0.5287	1.1047		
B_i^{P}	0.6558	1.058	1.5926	0.0012	1.8805	0.0297	1.1472		
$\%E_v$	36.33	50.70	54.97	73.53	35.49	44.30			
					$Z = -\text{N}_2\text{C}_3\text{H}_3$				
B_i^{R}	0.0044	1.7033	1.055	0.7962	1.0082	0.9108	0.9799	0.5061	0.8550
B_i^{ET}	0.2322	1.3793	1.4463	0.1902	1.324	0.5304	0.8492		
B_i^{P}	0.6471	1.0754	1.6994	0.0012	1.8771	0.0332	0.9896		
$\%E_v$	35.44	51.60	60.72	76.23	36.34	43.35			

$Z = \text{NH}_2, \text{N}(\text{CH}_3)_2, \text{NHOH}$, and $\text{N}_2\text{C}_3\text{H}_3$.

Wiberg bond indexes (B_i), % evolution through the reaction coordinate ($\%E_v$), average bond index variation (δB_{av}), and synchronicity parameter (S_y) are shown.

vessel was seasoned with the product of decomposition of allyl bromide at high temperature to produce a polymeric coat in the reaction vessel. The rate coefficients were determined manometrically. The temperature was found to be within $\pm 0.2^\circ\text{C}$ when controlled by a SHINKO DIC-PS 23TR resistance thermometer controller with a calibrated iron–constantan thermocouple. Then, the temperature lecture is measured within $\pm 0.1^\circ\text{C}$ with a thermopar of iron–constantan attached to a Digital Multimeter Omega 3465B. The reaction vessel showed no temperature gradient at different points, and the substrate was injected directly into the reaction vessel through a silicone rubber septum.

CONCLUSIONS

The experimental data show that the elimination process of N-substituted *tert*-butyl carbamates in the gas-phase is homogeneous, unimolecular, and follows a first-order rate law.

Theoretical calculations of these reactions suggest it proceeds through a concerted asynchronous mechanism. The TS structure of the rate-determining step for the gas-phase elimination of N-substituted *t*-butyl carbamates is a six-member ring geometry with some departure from planarity when the nitrogen of the carbamates bears bulky substituents. We demonstrate that the hydrogen is abstracted by the carbonyl oxygen, not by the amide nitrogen. In the TS structure the hydrogen is located halfway between the carbonyl oxygen and alkyl beta carbon. Calculated activation parameters are in good agreement with experimental values at B3LYP/6-31G(d,p) level of theory. Analysis of NBO charges and bond orders suggests that the polarization of alkyl oxygen–carbon bond, in the sense $\text{O}^{\delta-}-\text{C}\alpha^{\delta+}$, is the determining factor in the decomposition process, with this reaction coordinate being the most advanced for all substrates in the TS. The presence of an aromatic system and electron withdrawing groups in the carbamate nitrogen facilitates the decomposition process by polarizing the alkyl carbon–oxygen bond; nonetheless other factors such as steric constraints and loss of entropy may also be important, in view of the fact that the more constrained TS correspond to the fastest reaction.

REFERENCES

- Daly NJ, Ziolkowski F. *Aust. J. Chem.* 1971; **24**: 2541–2546.
- Thorne MP. *J. Chem. Soc.* 1978; 715–718.
- Taylor R. In *The Chemistry of Functional Groups, Supplementary Volume B, Acid Derivatives* (Chap. 15), Patai S (ed.). Wiley: Chichester, 1979.
- Holbrook KA. In *The Chemistry of Acids Derivatives, Volume 2, Vapor and Gas Phase Reactions of Carboxylic Acids and Their Derivatives* (Chap. 12), Patai S (ed.). Wiley: Chichester, 1992.
- Smith GG, Voorkees KI, Kelly FM. *J. Chem. Soc. Chem. Comm.* 1971; 789.
- Gordon AS, Norris WP. *J. Phys. Chem.* 1965; **69**: 3013–3017.
- H. Kwart H, Slutsky J. *J. Chem. Soc. Chem. Comm.* 1972; 552–553.
- Daly NJ, Heweston GW, Ziolkowsky F. *Aust. J. Chem.* 1973; **26**: 1259–1262.
- Kwart H, Slutsky J. *J. Chem. Soc. Chem. Comm.* 1972; 1182–1183.
- Herize A, Domínguez RM, Rotinov A, Nuñez O, Chuchani G. *J. Phys. Org. Chem.* 1999; **12**: 201–206.
- Daly NJ, Ziolkowsky F. *J. Chem. Soc. Chem. Commun.* 1972; 911–912.
- M. Luiggi M, Domínguez RM, Rotinov A, Herize A, Cordova M, Chuchani G. *Int. J. Chem. Kinet.* 2002; **34**: 1–5.
- (a) Hansch C, Leo AJ. *Substituent Constants for Correlation Analysis in Chemistry and Biology*. Wiley: USA, 1979;; (b) Hansch C, Leo AJ, Taft R. *Chem. Rev.* 1991; **91**: 165–195.
- Chuchani G, Nuñez O, Marciano N, Napolitano S, Rodríguez H, Domínguez M, Ascanio J, Rotinov A, Domínguez RM, Herize A. *J. Phys. Org. Chem.* 2001; **14**: 146–158.
- Chuchani G, Domínguez RM, Rotinov A, Herize A. *J. Phys. Org. Chem.* 1999; **16**: 40–46.
- Ruiz Gonzalez JM, Loroño M, Cordova T, Chuchani G. *J. Mol. Struct.: Theochem* 2005; **732**: 56–61.
- Brusco Y, Domínguez RM, Rotinov A, Herize A, Cordova M, Chuchani G. *J. Phys. Org. Chem.* 2002; **15**: 796–800.
- Graterol M, Cordova T, Chuchani G. *J. Phys. Org. Chem.* 2006; **19**: 700–705.
- Frisch MJ, Trucks GW, Schlegel HB, Scuseria GE, Robb MA, Cheeseman JR, Zakrzewski VG, Montgomery JA, Jr, Stratmann RE, Burant JC, Dapprich S, Millam JM, Daniels AD, Kudin KN, Strain MC, Farkas O, Tomasi J, Barone V, Cossi M, Cammi R, Mennucci B, Pomelli C, Adamo C, Clifford S, Ochterski J, Petersson GA, Ayala PY, Cui Q, Morokuma K, Malick DK, Rabuck AD, Raghavachari K, Foresman JB, Cioslowski J, Ortiz JV, Stefanov BB, Liu G, Liashenko A, Piskorz AP, Komaromi I, R. Gompert R, Martin RL, Fox DJ, Keith T, M Al-Laham MA, Peng CY, Nanayakkara A, Gonzalez C, Challacombe M, P. Gill PMW, Johnson B, Chen W, Wong MW, Andres JL, Head-Gordon M, Replogle ES, Pople JA. Gaussian 98, Revision A.3, Gaussian, Inc., Pittsburgh, PA, 1998.
- McQuarrie D. *Statistical Mechanics*. Harper & Row: New York, 1986.
- Foresman JB, Frish AE. *Exploring Chemistry With Electronic Methods* (2nd edn). Gaussian, Inc.: Pittsburg, PA, 1996.
- Benson SW. *The Foundations of Chemical Kinetics*. Mc-Graw-Hill: New York, 1960.
- Rotinov A, Dominguez RM, Córdoba T, Chuchani G. *J. Phys. Org. Chem.* 2005; **18**: 616–624.
- (a) O'Neal HE, Benson SW. *J. Phys. Chem.* 1967; **71**: 2903–2921; (b) Benson SW. *Thermochemical Kinetics*. John Wiley & Sons: New York, 1968.
- Lendvay G. *J. Phys. Chem.* 1989; **93**: 4422–4429.
- Reed AE, Weinstock RB, Weinhold F. *J. Chem. Phys.* 1985; **83**(2): 735–746.
- Reed AE, Curtiss LA, Weinhold F. *Chem. Rev.* 1988; **88**: 899–926.
- Wiberg KB. *Tetrahedron* 1968; **24**: 1083–1095.
- Gaussian NBO version 3.1.
- Moyano A, Periclas MA, Valenti E. *J. Org. Chem.* 1989; **54**: 573–582.
- Maccoll A. *J. Chem. Soc.* 1955; 965–973.
- Swinbourne E. *Aust. J. Chem.* 1958; **11**: 314–330.
- Domínguez RM, Herize A, Rotinov A, Alvarez-Aular A, Visbal G, Chuchani G. *J. Phys. Org. Chem.* 2004; **17**: 399–408.